IL NUOVO CIMENTO Vol. 37 C, N. 4 Luglio-Agosto 2014
DOI 10.1393/ncc/i2014-11799-9

Communications: SIF Congress 2013

Unusual nighttime impulsive enhancements of electron density characterizing the low-latitude ionosphere: Phenomenology and possible mechanisms of triggering

M. Pezzopane(*)
Istituto Nazionale di Geofisica e Vulcanologia - Roma, Italy

ricevuto il 7 Gennaio 2014; approvato il 19 Febbraio 2014

Summary. — Unusual nighttime impulsive electron density enhancements that are rarely observed at low latitudes on a wide region of South America are here investigated. These phenomena are very atypical because besides being of brief duration, they are characterized by a pronounced compression of the ionosphere. The events were studied and analyzed using both the F2 layer critical frequency (foF2) and the lowest virtual height of the ordinary trace of the F region (h'F) values recorded at five ionospheric stations widely distributed in space. A careful analysis of isoheight ionosonde plots suggests that traveling ionospheric disturbances (TIDs) caused by atmospheric gravity wave (AGW) propagation could play a significant role in causing these phenomena, both for quiet and for medium-high geomagnetic activity; in the latter case however a nocturnal recharging of the fountain effect, due to electric fields penetrating from the magnetosphere, plays an as much significant role.

PACS 94.20.dt – Equatorial ionosphere.
PACS 94.20.wg – Ionosphere/atmospheric interactions.
PACS 94.30.lr – Magnetic storms, substorms.
PACS 94.20.wh – Ionosphere/magnetosphere interactions.

1. – Introduction

In a region extending from a height of about 50 km to over 500 km, called *ionosphere*, some of the molecules of the atmosphere are ionized by the radiation coming from the Sun to produce an ionized gas. Ionization is the process in which electrons are removed from (or attached to) neutral atoms or molecules to form positively (or negatively) charged ions and free electrons. It is the ions that give their name to the ionosphere, but it is

(*) On behalf of L. Perna, E. Zuccheretti, P. R. Fagundes, R. de Jesus, M. A. Cabrera and R. G. Ezquer. E-mail: michael.pezzopane@ingv.it

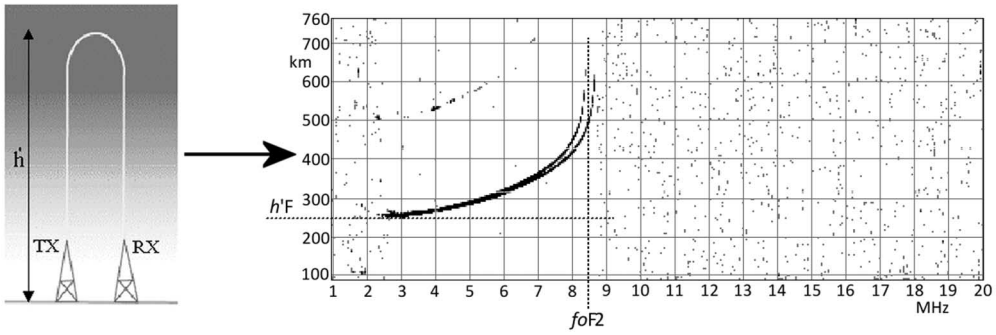

Fig. 1. – Example of ionogram recorded at Tucumán, Argentina, after performing a vertical sounding. The splitting of the trace (on the left the so-called ordinary ray and on the right the so-called extraordinary ray) is the result of the anisotropy characterizing the ionospheric plasma and due to the presence of the geomagnetic field. The vertical and horizontal dashed lines highlight, respectively, how the F2 layer critical frequency (foF2) and the lowest virtual height of the ordinary trace of the F region (h'F) are scaled.

the much lighter and more freely moving electrons which are important in terms of high-frequency electromagnetic propagation. Generally, the greater the number of electrons, the higher the frequencies that can be used. Ground-based ionospheric observations are mainly performed by a high-frequency radar known as *ionosonde*. The ionosonde sends short pulses of radio energy vertically into the ionosphere. These pulses are reflected back towards the ground and the ionosonde records the time delay between transmission and reception of pulses. By varying the carrier frequency of pulses typically from 1 to 20 MHz, the time delay at different frequencies is recorded. This record is referred to as *ionogram* and is usually presented in the form of a graph, where normally in place of time delay the virtual height is plotted according to the following equation:

$$\Delta t = \frac{2}{c} \cdot h', \tag{1}$$

where Δt is the time delay, h' is the virtual height and c is the free-space speed of the electromagnetic wave (fig. 1). The virtual height h', at a specified frequency of the pulses, is then the distance that a radio wave would have traveled at that frequency in half the elapsed time, $\Delta t/2$, at the free-space speed c. From the analysis of one ionogram several important ionospheric characteristics can be found (fig. 1) that have a significant role in the studies concerning ionospheric physics and related phenomena. The most important one is the F2 layer critical frequency (foF2) which is related to the electron density maximum (NmF2) of the ionosphere by the following expression:

$$Nm\mathrm{F2} = 1.24 \cdot 10^{10} \cdot (fo\mathrm{F2})^2, \tag{2}$$

where the units of NmF2 and foF2 are electrons/m^3 and MHz, respectively.

The foF2 measured values often show a significant deviation from long-term values. Many studies have been made to unveil any trends of these deviations as a function of local time, season, and solar/geomagnetic activity (see, *e.g.*, [1-3]). Additionally to F2

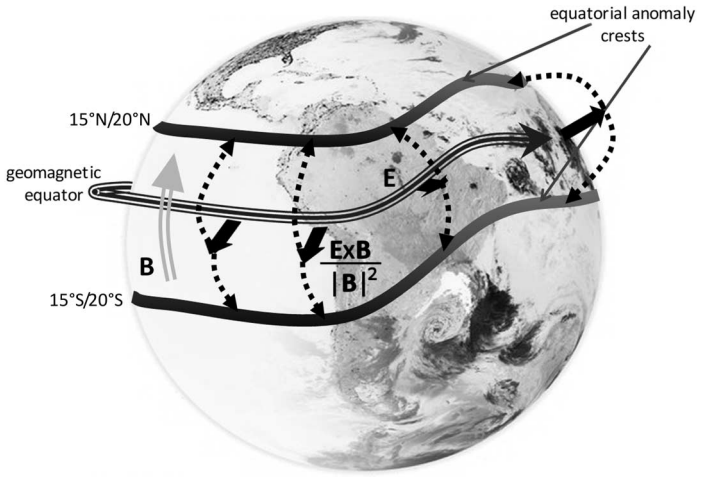

Fig. 2. – Sketch of the "equatorial fountain effect". Latitudes are geomagnetic.

layer instabilities caused by solar and geomagnetic activity variations, there are however disturbances, termed "meteorological" [4], appearing from the lower part of the atmosphere and hence considered different from those caused by the solar/geomagnetic activity.

This paper is focused on the analysis of very unusual and rare events characterizing the F2 layer, called "impulsive electron density enhancement" because a sudden large increase in electron density is immediately followed by an equally rapid recovery phase. Moreover, the phenomenon is distinguishing because it corresponds to a pronounced compression of the ionospheric layer. The events under study were recorded on a wide region of South America, below the southern crest of the equatorial anomaly, which is a very distinctive region. In fact, at equatorial latitudes, and quite precisely at the geomagnetic equator, the geomagnetic field $\mathbf{B}$ is nearly parallel to the Earth's surface, and, during daytime, the ionospheric E region is characterized by an eastward dynamo electric field $\mathbf{E}$. The resulting $(\mathbf{E} \times \mathbf{B})/|\mathbf{B}|^2$ drift transports plasma upward till it moves along the geomagnetic field lines in response to gravity and pressure-gradient forces. As a result, the daytime equatorial ionosphere presents a minimum of ionization density at the geomagnetic equator and maxima at the two crests, approximately 15°–20° in geomagnetic latitude to the north and south. This low-latitude ionospheric feature is called "equatorial anomaly" and the corresponding triggering electrodynamic mechanism is known as the "equatorial fountain effect" (fig. 2). The nighttime E region dynamo electric field is instead westward, and less evident because the electron density is smaller, then the drift turns downward and the fountain becomes a reverse fountain with a flow of ionization from both hemispheres.

This paper is based on the analysis of all the nighttime impulsive electron density enhancements recorded from August 2007, when an Advanced Ionospheric Sounder by Istituto Nazionale di Geofisica e Vulcanologia (AIS-INGV) ionosonde was installed at Tucumán (TUC) (26.9°S, 65.4°W, geom. Lat. 16.8°S), Argentina [5], to January 2012. In this period of time the phenomenon under investigation was recorded only ten times and specifically, two events, occurred respectively for quiet and disturbed geomagnetic

conditions, are deeply analyzed in this paper to look into the differences characterizing the possible mechanisms of triggering.

2. – Data

In order to detect the peculiar *fo*F2 nighttime impulsive enhancements that occurred from August 2007 to January 2012, the visualization feature of the electronic Space Weather upper atmosphere (eSWua) database (`http://www.eswua.ingv.it/`) [6] was exploited, simply by checking the daily *fo*F2 plots computed on the basis of the values produced automatically as output by Autoscala [7-9] from the ionograms recorded at Tucumán. The analysis was then based also on data recorded from four additional ionosondes: Sao Luis (SL) (2.6°S, 44.2°W, geom. Lat. 6.2°N), Cachoeira Paulista (CP) (22.4°S, 44.6°W, geom. Lat. 13.4°S), São José dos Campos (SJC) (23.2°S, 45.9°W, geom. Lat. 14.1°S), Brazil, and Jicamarca (JIC) (12.0°S, 76.8°W, geom. Lat. 2.0°S), Peru. The level of geomagnetic activity characterizing the events under study is indicated by the 3 hourly-Kp, AE, and Dst indices, which were downloaded from the World Data Center for Geomagnetism, Kyoto, Japan through the site `http://wdc.kugi.kyoto-u.ac.jp/`.

3. – Results

Upper panels of fig. 3 show two atypical *fo*F2 enhancements that were recorded at Tucumán on 8 September 2010 ($Kp_{max} = 3$, $Dst_{max} = -35\,\mathrm{nT}$, $AE_{max} = 210\,\mathrm{nT}$) and 7 April 2011 ($Kp_{max} = 6$, $Dst_{max} = -60\,\mathrm{nT}$, $AE_{max} = 1176\,\mathrm{nT}$). In particular, all the ionograms recorded for all the month including each event were considered and validated according to the International Union of Radio Science (URSI) standard [10]. Once the scaled *fo*F2 values had been obtained, the corresponding monthly mean and standard deviation were calculated. Both events show a significant and rapid (less than 2 h) increase in *fo*F2 beginning at about 05:00 universal time (UT) (local time (LT) = UT − 4), whose peak values are well outside the confidence interval defined by the standard deviation and 50% higher of the mean value. The phenomenon is extremely impulsive, and the bell-shaped trend of the *fo*F2 plot is very narrow, because after reaching a peak, the *fo*F2 falls to very low values and the decrease phase is even more rapid (about 1 h) than the increase phase. Central panels of fig. 3 show the same plots for the lowest virtual height of the ordinary trace of the F region (h'F), and the most remarkable feature emerging by comparing the *fo*F2 and the h'F plots is that when *fo*F2 presents an impulsive enhancement and reaches its maximum value, the ionosphere is strongly compressed, with the minimum value of h'F either well outside or very close the lower bound of the confidence interval defined by the standard deviation. This suggests that a nighttime recharging of the fountain effect and/or a downward plasma diffusion from the plasmasphere cannot be considered as the only agents responsible for the event, and that something like a travelling ionospheric disturbance (TID) might have played a substantial role [11]. In order to look for the possible presence of TIDs caused by atmospheric gravity wave (AGW) propagation, the ionogram traces recorded at Tucumán from 00:00 to 10:00 UT for both the identified events were manually digitized, obtaining a sequence of couples of values (N, h') for each ionogram, where N is the electron density and h' is the virtual height of reflection. Then, inversion from the ionogram trace (N, h') to the profile (N, h), where h is the real height of reflection, was performed using the POLAN technique [12]. From the profiles (N, h) isoheight curves (from $h = 170\,\mathrm{km}$ to $h = 300\,\mathrm{km}$, with a step of 10 km) of N were obtained (lower panels of fig. 3) showing that for both the considered days maxi-

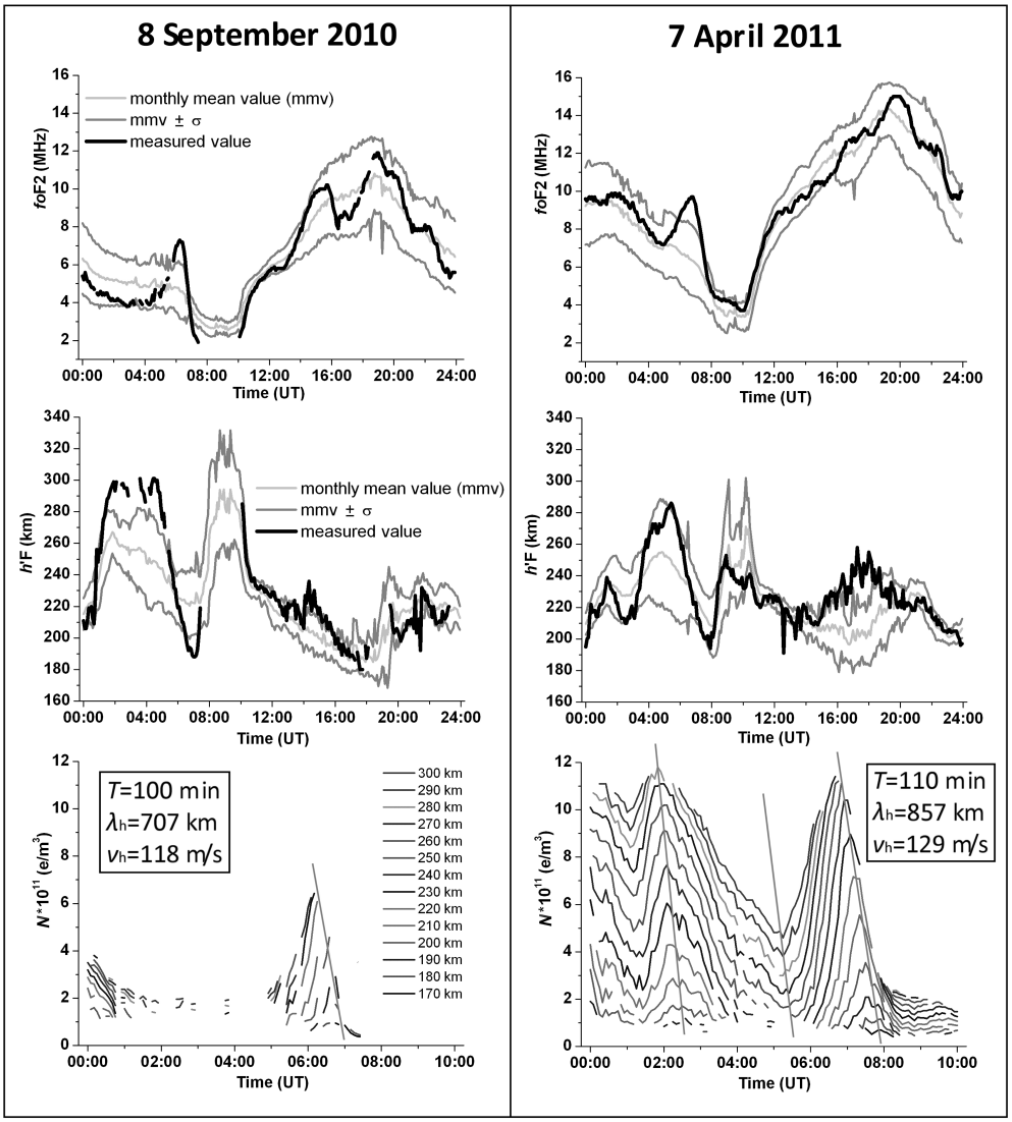

Fig. 3. – The (upper panels) foF2 and (central panels) h'F plots obtained at Tucumán on 8 September 2010 and 7 April 2011. The lower panels show for the same dates the electron density variations for the real height range 170–300 km from 00:00 to 10:00 UT; oblique lines highlight the downward phase shift propagation typical of AGW propagation, whose main parameters estimated from the isoheight curves are also shown.

mum N variations occur first at higher altitudes and then at lower altitudes, highlighting a downward phase shift which is characteristic of AGW propagation (see fig. 4).

Using isoheight curves shown in fig. 3, it is possible to estimate the AGW period T; the vertical phase velocity v_z is calculated using the peak of two consecutive heights (see fig. 5 of [13]), the vertical wavelength $\lambda_z = v_z T$ is then obtained. The corresponding horizontal wavelength (λ_h) can be determined using a relationship between λ_h and λ_z,

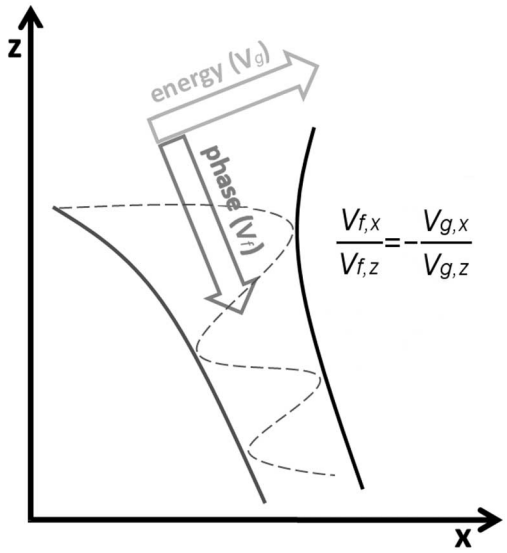

Fig. 4. – Geometry characterizing the group velocity ($\mathbf{V}_g$) and the phase velocity ($\mathbf{V}_f$) of an atmospheric gravity wave.

namely, $\omega^2\lambda_h^2 \approx (\omega_g^2 - \omega^2)\lambda_z^2$ [14], where ω_g is the BruntVäisälä frequency, which was taken as $2\pi/14\,\mathrm{min}^{-1}$ [15], and $\omega = 2\pi/T$ is the wave angular frequency. Lower panels of fig. 3 list the estimates of the wave parameters T, λ_h and v_h for both the events as inferred from the isoheight plots; with regard to the horizontal wavelength values, these are consistent with medium-scale TIDs (MSTIDs) [16].

In order to investigate the spatial extent of the unusual nighttime *fo*F2 impulsive enhancements detected at Tucumán, fig. 5 shows the *fo*F2 plots obtained at different ionospheric stations for both events. Unfortunately, on 8 September 2010 at SJC from 02:00 to 06:00 UT (LT = UT − 3) the ionograms were characterized by spread F phenomena and it was impossible to obtain a value for *fo*F2. Figure 5b shows that on 8 September 2010, even though less pronounced, an electron density increase also occurs at CP (LT = UT − 3), and the fact that the *fo*F2 plot obtained at SL (LT = UT − 3) does not exhibit any enhancement (see fig. 5a) also highlights how the event is for this day confined around the southern anomaly crest. Moreover, when *fo*F2 undergoes an impulsive enhancement at TUC, the analysis of h'F plots (figures not shown here) shows that the ionosphere, besides TUC, is strongly compressed also at CP and SJC, while at SL the h'F trend does not exhibit any significant feature. Figures 5a-d are representative and present the same characteristics of all the other cases occurred for low and medium geomagnetic activity (figures not shown here). Concerning the case recorded on 7 April 2011, occurred for medium-high geomagnetic activity, figs. 5f-g show that, even though less pronounced, an electron density increase occurs also at CP and SJC. However, for this event an electron density increase is observed also at the geomagnetic equator, specifically at JIC (LT = UT − 5) (fig. 5e); hence, contrarily to what observed on 8 September 2010, in this case the event is not confined around the southern anomaly crest. Moreover, the analysis of h'F plots (figures not shown here) shows that the ionosphere at TUC, SJC, and slightly at CP, is compressed, while at JIC this compression is not perceivable.

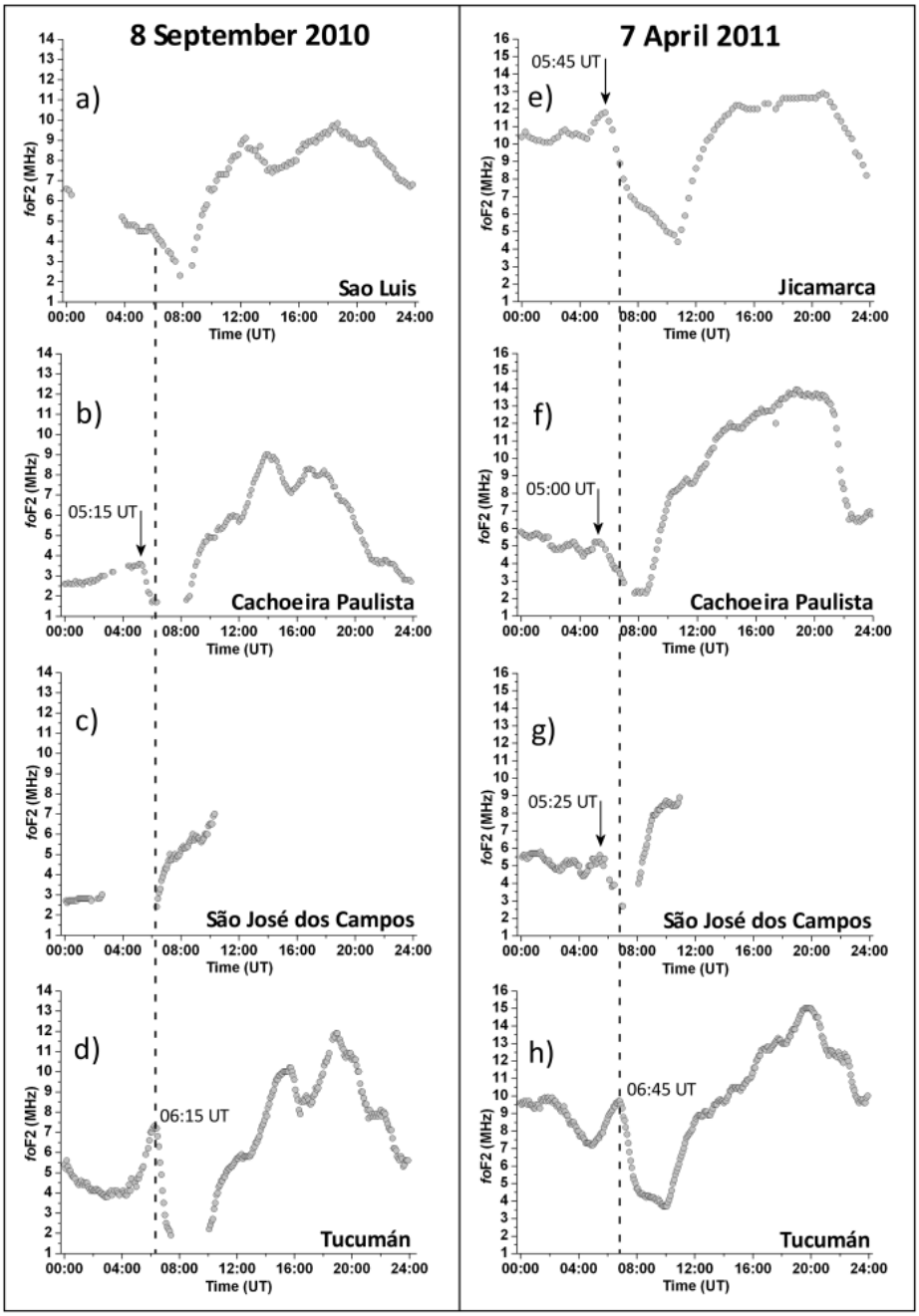

Fig. 5. – The *fo*F2 plots obtained at (left column) SL, CP, SJC, and TUC on 8 September 2010 and at (right column) JIC, CP, SJC, and TUC on 7 April 2011. The vertical dashed line highlights the occurrence time of the electron density enhancement maximum recorded at Tucumán. Down arrows highlight the occurrence time of the electron density enhancement maximum at the ionospheric stations different from Tucumán.

4. – Discussion and conclusions

Using ground based measurements in the South American region, it was shown that the equatorial ionosphere rarely suffers a significant and atypical nighttime modification showing the following main features: 1) impulsive post-midnight enhancement of *fo*F2 recorded at some ionospheric stations widely distributed in space; 2) strong compression of the ionosphere; 3) for quiet and medium geomagnetic conditions the enhancement is recorded only by those stations located around the southern crest of the equatorial anomaly; 4) for medium-high geomagnetic conditions the enhancement is recorded also by those stations located at the geomagnetic equator, indicating a recharging of the fountain effect.

Several authors (*e.g.*, [17]) agree on the explanation that the observed post-midnight *fo*F2 enhancements are due either to the equatorward thermospheric winds, along with a nighttime plasmaspheric flux into the F region, or to a recharging of the fountain effect, both mechanisms being characterized by an uplifting of the F region. Hence, these explanations cannot be considered satisfactory for the events dealt with in this paper, because the impulsive enhancements of *fo*F2 illustrated in fig. 3 are associated with a definite compression of the F region. On the other hand, recently it was found that this anticorrelation can be explained in terms of the positive/negative vertical shear, due to TIDs caused by upward AGW propagation [11]. According to this and to the evidence that MSTIDs can propagate also equatorward of the equatorial crests [18], the dashed straight line in fig. 6 represents the wavefront of a MSTID propagating in the northwest direction on 8 September 2010, coherently with the fact that the *fo*F2 enhancement recorded is observed before at CP and approximately 1 h later at TUC, and after assuming a distance between CP and TUC along the propagation direction of about 400 km, which is consistent with the wave parameters shown in fig. 3. Concerning the event occurred on 7 April 2011, fig. 5 shows that, unlike the event recorded on 8 September 2010, an impulsive increase of *fo*F2 was recorded also at the geomagnetic equator, at JIC, at 05:45 UT, about one hour prior to the enhancement recorded at TUC. Moreover, the increase recorded at JIC is not associated with an ionospheric compression, this being an evidence that in this case a nocturnal recharging of the fountain effect occurred and played an important role in causing the phenomenon under study; this recharging can be due to either a zonal electric field reversal or a decreasing westward electric field [19], that are generally caused by penetrating interplanetary electric fields (IEFs) of magnetospheric origin, especially for disturbed geomagnetic conditions [20]. The times of occurrence of the peaks recorded at CP and SJC (45 and 20 min before than the one observed at JIC) indicate that they are not correlated with the electron density increase recorded at JIC. Moreover, these two peaks are associated with a compression of the ionosphere (figures not shown here) implying that also in this case TIDs should be taken into account to explain the phenomenon. Hence, similarly to what it was just previously done for the event occurred on 8 September 2010, the continuous straight line in fig. 6 illustrates the wavefront of a MSTID propagating in the northwest direction on 7 April 2011; this is coherent with the fact that the *fo*F2 enhancement is observed before at SJC and approximately 1 h and 20 min later at TUC, assuming for the MSTID the wave parameters shown in fig. 3, and a distance of about 600 km between TUC and SJC along the propagation direction. The same scenario accounts pretty well also for the delays of 25 min between CP and SJC and 1 h and 45 min between CP and TUC. Therefore, an important result reached by this study is that, independently of the geomagnetic activity, AGW propagation plays without doubt a significant role in causing these anomalous postmidnight electron density

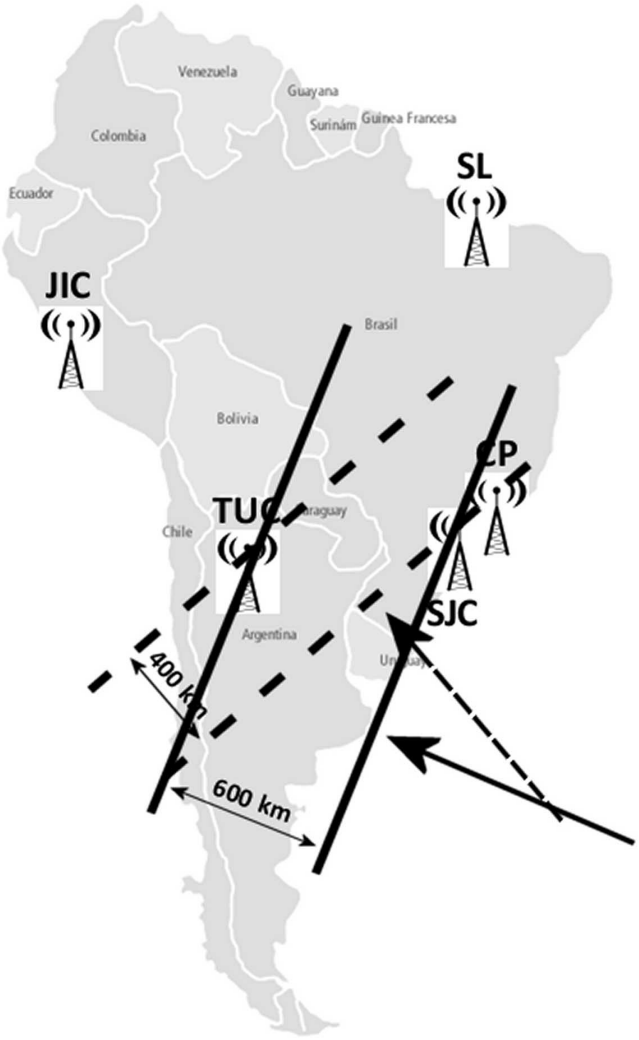

Fig. 6. – Wavefront of a medium-scale traveling ionospheric disturbance (MSTID) propagating northwestward in the Southern Hemisphere on (dashed line) 8 September 2010 and (continuous line) 7 April 2011. The locations of the five ionospheric stations considered in the study are also highlighted.

increases characterizing the low-latitude ionosphere.

Finally, the amplification of the phenomenon recorded at TUC could be attributed to the different behavior generally shown by different ionospheric longitudinal sectors [21]. For medium-high geomagnetic conditions, this amplification could also be due to the fact that the longitudinally dependent recharging of the fountain effect, probably caused by penetrating IEFs, progressively adds up to the northwestward MSTID caused by AGW propagation. With regard to this, this study suggests that values of $AE > 1000\,\mathrm{nT}$ and $Kp > 5$ are necessary to trigger a nocturnal recharging of the fountain effect contributing to the anomalous electron density enhancements investigated in this work.

REFERENCES

[1] Mikhailov A. V., Perrone L. and Smirnova N. V., *J. Atmos. Sol.-Terr. Phys.*, **51** (2012) 59.
[2] Adeniyi J. O. and Ikubanni S. O., *Adv. Space Res.*, **51** (2013) 1709.
[3] Pavlov A. V. and Pavlova N. M., *Adv. Space Res.*, **51** (2013) 2018.
[4] Rishbeth H. and Mendillo M., *J. Atmos. Terr. Phys.*, **63** (2001) 1661.
[5] Pezzopane M., Zuccheretti E., Bianchi C., Scotto C., Zolesi B., Cabrera M. A. and Ezquer R. G., *Ann. Geophys. Italy*, **50** (2007) 483.
[6] Romano V., Pau S., Pezzopane M., Zuccheretti E., Zolesi B., De Franceschi G. and Locatelli S., *Ann. Geophys.*, **26** (2008) 345.
[7] Pezzopane M., Scotto C., Tomasik L. and Krasheninnikov I., *Acta Geophys.*, **58** (2010) 513.
[8] Pezzopane M. and Scotto C., *Comp. Geosci.*, **36** (2010) 1168.
[9] Scotto C. and Pezzopane M., *J. Atmos. Sol.-Terr. Phys.*, **70** (2008) 1929.
[10] Wakai N., Ohyama H. and Koizumi T., *Manual of Ionogram Scaling*, 3rd version, report, (Radio Research Laboratory, Ministry of Posts and Telecommunication, Tokyo) 1987.
[11] Lu G., Richmond A. D., Roble R. G. and Emery B. A., *J. Geophys. Res.*, **106** (2001) 493.
[12] Titheridge J. E., *Radio Sci.*, **23** (1988) 831.
[13] Cabrera M. A., Pezzopane M., Zuccheretti E. and Ezquer R. G., *Ann. Geophys.*, **28** (2010) 1133.
[14] Hines C. O., *Can. J. Phys.*, **38** (1960) 1441.
[15] Abdu M. A., Batista I. S., Kantor I. J. and Sobral J. H. A., *J. Atmos. Terr. Phys.*, **44** (1982) 759.
[16] Leitinger R. and Rieger M., *Ann. Geophys. Italy*, **48** (2005) 515.
[17] Liu L., Chen Y., Le H., Ning B., Wan W., Liu J. and Hu L., *J. Geophys. Res. Space Phys.*, **118** (2013) 4640.
[18] Makela J. J., Miller E. S. and Talaat E. R., *Geophys. Res. Lett.*, **37** (2010) L24104.
[19] Nicolls M. J., Kelley M. C., Vlasov M. N., Sahai Y., Chau J. L., Hysell D. L., Fagundes P. R., Becker-Guedes F. and Lima W. L. C., *Ann. Geophys.*, **24** (2006) 1317.
[20] Zhao B., Wan W., Liu L., Igarashi K., Nakamura M., Paxton L. J., Su S.-Y., Li G. and Ren Z., *J. Geophys. Res.*, **113** (2008) A11302.
[21] Pezzopane M., Zuccheretti E., Abadi P., De Abreu A. J., De Jesus R., Fagundes P. R., Supnithi P., Rungraengwajiake S., Nagatsuma T., Tsugawa T., Cabrera M. A. and Ezquer R. G., *Ann. Geophys.*, **31** (2013) 153.